SEISMIC CHARACTERIZATION OF THE QUATERNARY SEDIMENTS AT LLANCANELO-LAKE AREA, ARGENTINA

JOSÉ M. CARCIONE[1], MATÍAS DE LA VEGA[2], DAVIDE GEI[1], ANA OSELLA[2], STEFANO PICOTTI[1], ALEJANDRO TASSONE[3] and MAURIZIO POSCOLIERI[4]

[1] *Istituto Nazionale di Oceanografia e di Geofisica Sperimentale (OGS), Borgo Grotta Gigante 42c, 34010 Sgonico, Trieste, Italy. jcarcione@inogs.it*
[2] *Departamento de Física, Facultad de Ciencias Exactas y Naturales, Universidad de Buenos Aires - IFIBA Conicet, Ciudad Universitaria, Pab. 1, 1428 Buenos Aires, Argentina. osella@df.uba.ar*
[3] *INGEODAV, Departamento de Ciencias Geologicas, FCEyN, Universidad de Buenos Aires , Argentina.*
[4] *IDASC, Institute of Acoustics and Sensors "Orso Mario Corbino", Research Area of Rome Tor Vergata, Via del Fosso del Cavaliere 100, 00133 Roma, Italy.*

(Received July 16, 2012; revised version accepted November 5, 2012)

ABSTRACT

Carcione, J.M., de la Vega, M., Gei, D., Osella, A., Picotti, S., Tassone, A. and Poscolieri, M., 2013. Seismic characterization of the Quaternary sediments at Llancanelo-Lake area, Argentina. *Journal of Seismic Exploration*, 22: 1-18.

A preliminary near-surface seismic survey was carried out at Llancanelo Lake (Argentina) with the aim of mapping the quaternary layers, composed of sedimentary layers overlying basalt. A geological model has been obtained by interpreting the events of a common-shot gather. Expressions of the traveltimes of the direct and refracted waves versus offset provide means to evaluate the velocities of the layers and thickness of the upper layer. Moreover, the standard processing sequence is applied to the data to obtain a stacked section. This procedure reveals the location of deeper interfaces, although it is highly affected by the filtering of the direct and refracted events, which have the same slope of the medium- and far-offset reflection signals.

The fact that the direct arrival has not a zero intercept time indicates the presence of a very thin layer at the surface(shallow salt deposits). Further evidence of the near-surface layer is that the refracted and reflection events are ringing and there are strongly dispersive Rayleigh waves. An interface has been found approximately between 54 and 57 m depth. The P- and S-wave velocities of the shallow layer are 2000 and 550 m/s, according to the slopes of the direct and Rayleigh waves,

0963-0651/13/$5.00

respectively, and rock-physics empirical relations, while the lower layer has a P-wave velocity of 2800 m/s, obtained from the refracted event. A tentative interpretation of the apex of a reflection event locates the top of the basalt layer at 190 m depth approximately. A viscoelastic model has been defined, with quality factors of typical volcaniclastic sediments. We then compute a synthetic common-shot gather and snapshots by means of full-wave pseudospectral methods. The synthetic gather resembles the real one, providing additional support to the interpretation.

KEY WORDS: processing, modeling, waves, interpretation.

INTRODUCTION

Geoelectrical surveys were performed at the Llancanelo-Lake area (Argentina) to map the quaternary sedimentary layers and define the depth of the basalt layer (Violante et al., 2010; de la Vega et al., 2011). However, because of the highly conductive nature of the soil, it has been difficult to detect the top of the basalt layer. Due to this reason, we have acquired a preliminary seismic-reflection profile to verify the possibility of a better definition of the layers.

Llancanelo Lake is located in the Payenia volcanic province, which has an area of about forty thousand km^2, with approximately eight thousand km^3 of volcanic volume erupted during the last two million years. The area is situated at the province of Mendoza in the Andes region. The Quaternary Payenia was generated by the collapse of the San Rafael block in the Pleistocene due to the steepening of the subducted slab and the injection of hot asthenosphere material (Ramos and Folquera, 2011). The Payún Matru volcanic field is the more active at present.

In particular, the study of the Quaternary sediments at Llancanelo Lake and its surroundings is important from several points of view, i.e., from the geological-environmental aspects to the biological, paleontological, anthropological and archaeological aspects (Gil et al., 2005; Violante et al., 2010). Moreover, the area is appropriate to study the paleoclimate history, since the region has not been covered by ice during the glaciations, favouring the sedimentation and the preservation of cold climate sequences. The lake, which evolved under the action of volcanism and climate changes, was a regional depocenter during the Pliocene-Quaternary period. Therefore, it contains intra and extra basinal clastic and evaporitic sediments dominated by volcaniclastic products. Previous studies reveal the presence of a sedimentary sequence at least 30 m thick composed mainly of volcaniclastic sediments (Violante et al., 2010). There are embedded ash layers, evaporites and aeolian and swamp deposits. Geoelectrical surveys indicate that at the west coast of Llancanelo Lake there are no basalt layers in the upper 30 m, but basalt outcrops can be seen in the vicinities. The shallow and conductive sediment layers can be associated to the presence of the phreatic level, and the lower layers with more compacted

sediments and basalt. The lacustrine sediments seem to extend at least 2.5 km west from the coast, where palustrine deposits are present. Risso et al. (2008) provide a detailed stratigraphic column of the very shallow layers and outcrops.

Recently, de la Vega et al. (2011) performed additional geoelectrical surveys at Llancanelo Lake's surroundings. They recognized four main units, two of them of very high resistivity composed of basaltic lava flows and hence indicating the volcanic influence in the region, and the other two of very low resistivity corresponding to lacustrine sedimentary deposits. The upper lacustrine unit represents the last stages (Holocene) of evolution mainly dominated by climatic changes. The sediments represent saline, eolian and alluvial deposits. The area at the west side of the lake is covered by shallow salt deposits overlying paleo-lacustrine sediments. The aeolian deposits reach their maximum thickness at the eastern coast of the lake, where they constitute dunes several meters high. They are fine to very fine sands as well as silts, composed of gypsum and volcanic glass. The alluvial deposits cover the lowlands around Llancanelo Lake, and are composed of very fine sands, silts and clays of fluvial, lacustrine or evaporitic origin, with high amounts of volcaniclastic material.

In order to provide more evidence about the nature of the Quaternary sediments, we have acquired a multichannel seismic-reflection profile, with 37 common-shot gathers (see location in Fig. 1). The acquisition system, a Seismic Geometrics Geode DZ, consisted of 96 channels with a spacing of 10 m between receivers and variable distance between shots (10 to 50 m). The maximum fold is 24 and the sampling rate is 0.25 ms. The source was a shotgun impacting on the bottom of a shallow hole. A first interpretation is performed on a common-shot gather aided by forward seismic modeling. Then, we apply the standard processing sequence and obtain a stacked section.

INTERPRETATION OF A SINGLE COMMON-SHOT GATHER AND STACK

A common-shot gather acquired at the Payenia Volcanic Province, near Llancanelo lake (see Fig. 1), is shown in Fig. 2, where the distance between traces is 10 m. The stratigraphy is composed of Quaternary sediments of lacustrine origin overlying basalt (extrusive and therefore somewhat porous). The aerial view shows the survey region on the distal end of an alluvial fan. The sediments are clay rich and saturated with highly saline water. Sediments of this type are characterized by high porosity (greater than 40%), low density, low shear-wave velocity and high Poisson's ratio (greater than 0.4) (Mavko et al., 1998).

An interpretation of the various events is indicated, with only one refraction event clearly identified. In order to obtain information from these

events, we consider a single interface below the surface, although the final model will have a very thin shallow and unconsolidated layer. Any information about this layer is impossible to obtain from these data since receiver spacings less than half a meter would be necessary, although this layer is the reason why linear traveltime curves do not intercept the zero offset (Greenhalgh and King, 1981). The direct, refracted and reflected waves at depth h are shown in Fig. 3a and Fig. 3b shows the corresponding traveltime curves, whose expressions are given in the Appendix. The direct wave "D" is the P-wave traveling horizontally in the medium, but "D" may also represent similar straight events such as the Rayleigh wave, which travels with a velocity slightly less than that of the S-wave (for instance, the velocity is 0.92 times the shear velocity for a Poisson solid).

The "D" arrival has not a zero time intercept, but about 13 ms. This is due to the presence of the thin layer at the surface. A near-offset receiver spacing of 0.5 or 1 m would be necessary to observe this traveltime branch.

Fig. 1. Location of the seismic survey (square) at Mendoza, Argentina. The city of Malargüe and Llancanelo Lake are indicated.

Generally, there is always a 1 or 2 m thick, very low-velocity soil layer, which is under-saturated with water. Since its crossover must occur at offset less than 5 m, we can estimate a maximum P-wave velocity of 380 m/s and a thickness of about 2 m, with a good approximation. A Poisson's ratio of 0.25 or less would be expected for air-filled porosity, so we get v_S = 220 m/s. The porosity is almost certainly greater than 45%, so we assume a density of 1460 kg/m^3. Further evidence of the near-surface layer is that the refracted arrivals and near-surface reflection events are very ringing. This reverberation is typical of a low-velocity layer with a large impedance contrast at the bottom. Moreover, the high amplitude and strongly dispersive Rayleigh waves are characteristic of a near-surface low-velocity layer.

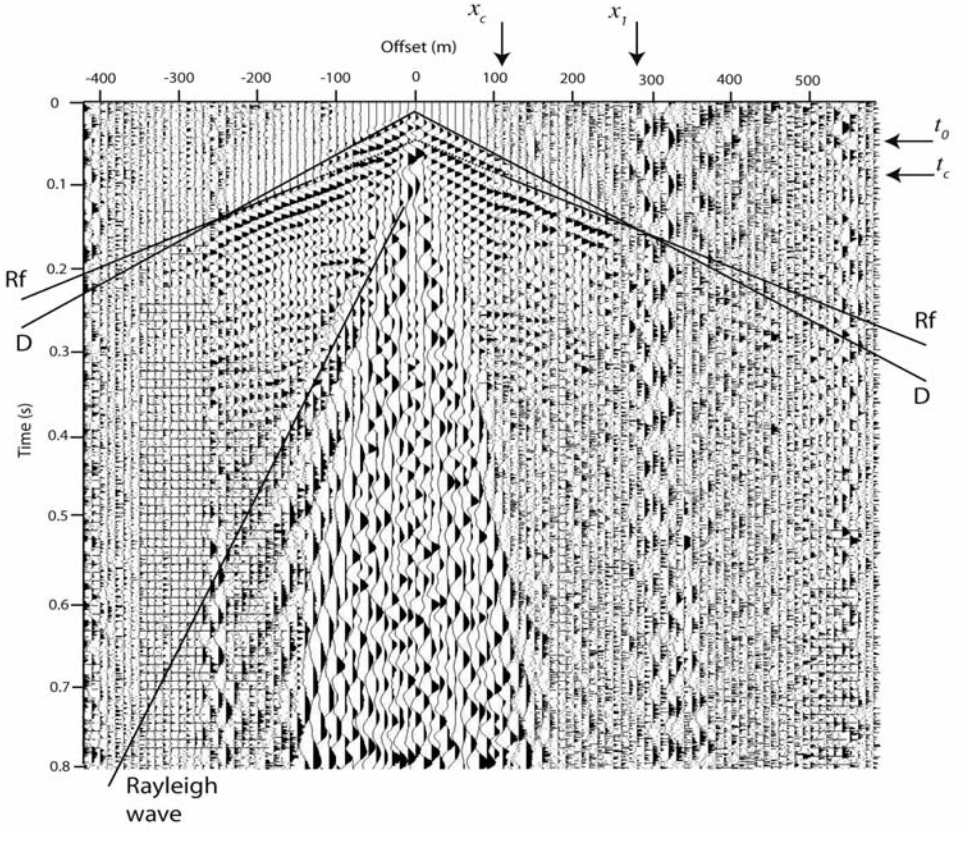

Fig. 2. Common-shot gather acquired at Payenia Volcanic Province near Llancanelo Lake. The various events are indicated and interpreted in Fig. 3. The expressions for the quantities, t_0-t_c, x_1 and x_c are given in eqs. (A-2), (A-3) and (A-4), respectively.

The period of the earlier events in Fig. 2 is approximately 0.02 s, which corresponds to a frequency of 50 Hz. In order to avoid spatial aliasing, the distance between stations has to satisfy

$$\Delta x \leq c/2f_{max} \quad , \tag{1}$$

where c is the velocity of the specific event and f_{max} is the maximum frequency of the signal. Assuming that the maximum frequency to preserve is 70 Hz, the proper sampling of the Rayleigh waves requires Δx to be approximately 4 m, if the velocity is 520 m/s (see below). Therefore, this event is aliased and this is the reason of its apparent low-frequency content.

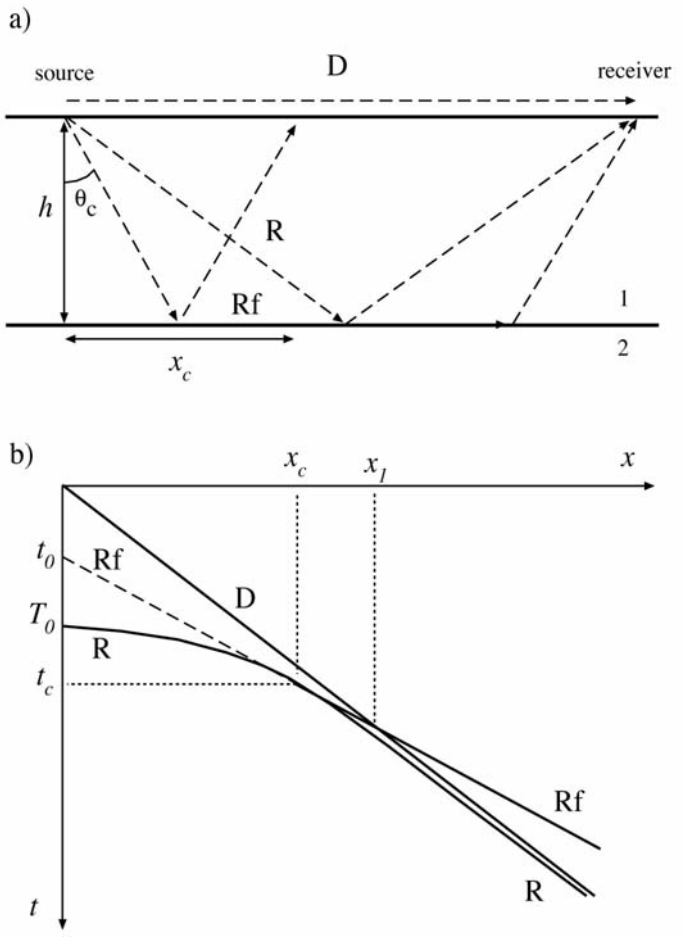

Fig. 3. Waves in the presence of a single interface below the surface. The interface separates medium 1 and 2. Direct (D), reflected (R) and refracted (Rf) waves (a) and corresponding traveltime curves (b).

Let us consider the traveltimes curves (see the Appendix). Snell's law at the critical angle can be written as

$$\sin\theta_c = v_1/v_2 \quad , \tag{2}$$

(e.g., Pilant, 1979), where θ_c is the critical angle and v_1 and v_2 are the P-wave velocities of the upper and lower layers. The refracted wave exists beyond this angle.

The values obtained from Fig. 2 are $t_0 = 0.04$ s, $t_c = 0.08$ s, $x_c = 110$ m and $x_1 = 280$ m. Then, the layer thickness calculated from eqs. (A-5) is 56.6 m, 57.1 m, 53.9 m and 57.1 m, respectively, which are very close together and provide confidence about the interpretation of the different events. The presence of this layer seems to confirm the interpretation of Violante et al. (2010), who found a layer of at least 30 m thickness composed of volcaniclastic sediments. The velocities obtained from the slopes of the direct and refracted waves yield $v_1 = 2000$ m/s and $v_2 = 2800$ m/s, while the Rayleigh wave velocity (assumed to be that of the fundamental mode) is approximately 520 m/s.

The normal-incidence two-way traveltime of the reflection event R is $T_0 = 0.056$ s if $h = 56$ m is assumed, and therefore, this event is masked by the direct and refracted waves. Other reflections events can be seen in Fig. 2 at negative offsets and beyond 0.1 s two-way traveltime. An hypothetical reflection hyperbola with apex at approximately $T_0 = 0.15$ s can be assumed, confirmed by the stack (see below). Thus, the depth of the second interface can be obtained from the expression

$$z_2 = h + v_2[(T_0/2) - (h/v_1)] \quad ,$$

which yields $z_2 = 188$ m.

On the basis of the Rayleigh-wave velocity we may assume a shear-wave velocity $v_S = 550$ m/s for the surface layer, since it can be shown that for a P-wave velocity $v_P = 2000$ m/s, the Rayleigh wave to S-wave ratio is 0.95 (e.g., Carcione, 2007). The apex of the hyperbola corresponding to the converted P-S wave at the first interface is expected at $T_0 = h[(1/v_1) + (1/v_S)] = 0.12$ s. Since the Rayleigh waves are spatially aliased, its use for phase-velocity estimation would be questionable. However, an alternative interpretation may support the assumed values. The surface layer is very porous, clay rich material with high Poisson's ratio. If we consider the Raymer-Hunt-Gardner velocity mixing relationship (see Mavko et al., 1998), we obtain a porosity of 42-43% and a density of 1960 kg/m^3. Application of the well-known mudrock line of Castagna (Mavko et al., 1998) gives $v_S = 550$ m/s and a Poisson's ratio of 0.46.

In order to perform the stack, we applied a 15-160 Hz bandpass filter and suppressed the ground roll in the f-k (frequency-wavenumber) domain (e.g., Yilmaz, 1989), since there is enough dip separation between these events and the reflection events. Fig. 4a shows a common-shot gather filtered in the f-k domain, where the Rayleigh waves have been removed. The primary reflection events and reflection multiples can be seen between 0.1 and 0.4 s two-way traveltime. We applied predictive deconvolution to selectively remove the reverberations caused by the shallow low-velocity layer. We designed the deconvolutional operator filter according to the Wiener-Levinson algorithm (Yilmaz, 1989), to sharpen seismic events and extend the frequency bandwidth. A mean autocorrelation is computed for a number of shots along all the seismic line in order to compute the average prediction lag (second zero crossing) and the average filter operator length (of the first autocorrelation transient). We used a prediction lag of 0.011 s and an operator length of 0.04 s. Fig. 4b clearly shows the effect of deconvolution on a shot after the f-k filter. The reverberation effect is almost completely removed from the data. We attempted to use a τ-p filter (Yilmaz, 1989) without success. We also apply an f-k filter to remove the refracted waves, although this process also removes part of the shallow reflection events as that generated at the first interface, and the medium- and far-offset part of deeper reflection events. However, this is necessary to avoid the stacking of refractions instead of reflections (Steeples and Miller, 1998). Then, we sorted the data from shot to common mid point (CMP) gathers,

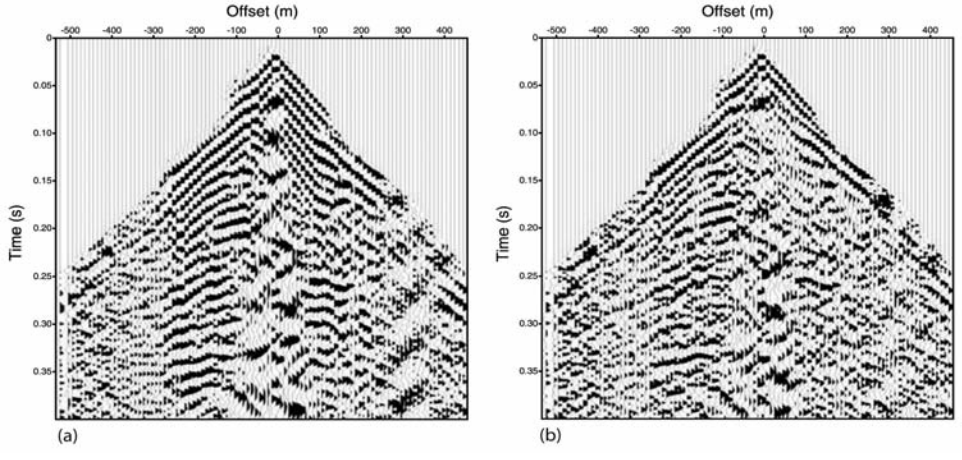

Fig. 4. f-k filtered common-shot, where the reflection events can be observed between 0.1 and 0.4 s propagation time (a), and after predictive deconvolution (b). The length of the prediction filter is 40 ms, while the prediction lag is 11 ms.

and performed a conventional stacking velocity analysis. We applied an f-x deconvolution to the final stack section, to improve the lateral coherence of the horizons.

Fig. 5 shows the stacked section with a tentative interpretation of the lateral variation of the seismic horizons. The first interfaces at approximately 50 ms confirms the interpretation of the single-shot seismogram, as well as the event marked at 150 ms, which can be related to the top of the basalt layer. Moreover, deeper reflection can be observed.

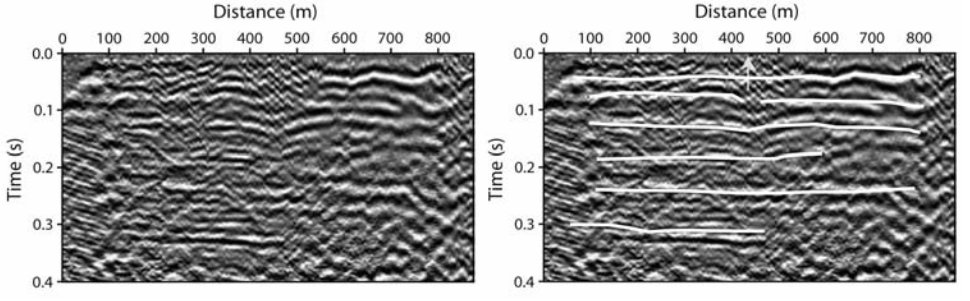

Fig. 5. Stacked seismic section without (left) and with (right) interpretation. The arrow indicates the location of the shot corresponding to the gather of Fig. 2.

SIMULATION OF A SYNTHETIC COMMON-SHOT GATHER

On the basis of the preceding interpretation, we build the model shown in Fig. 6, whose properties are given in Table 1, where v indicates the unrelaxed (high-frequency limit) velocities, and Q_P, Q_S and Q_k denote the P-wave, S-wave and dilatational quality factors, respectively (e.g., Carcione, 2007). Two thick volcaniclastic sediments layers overlay a basalt layer. Regarding layer 3, the Raymer-Hunt-Gardner and mudrock equations mentioned above yield a porosity of 37% and a Poisson's ratio of 0.38, with the properties reported in Table 1. Non-porous basalt has a density of 2950 kg/m^3 and $v_P \approx$ 7000 m/s. Since here we deal with extrusive basalts, this layer should have some porosity. The Wyllie time-average equation (Mavko et al., 1998) yields a porosity of 13% for v_P = 4800 m/s and the density would then be 2700 kg/m^3. This basalt layer is assumed to be a Poisson solid, i.e., $v_S = v_P/\sqrt{3}$.

The quality factors of all the layers are related to the velocities as $Q = v^{0.45}$, where v is given in m/s. The Q factors correspond to a frequency of 25 Hz, which is the dominant (central) frequency of the source, and agree with reported data for volcaniclastic sediments (e.g., Petrosino et al., 2002) and

preliminary calculation performed with the spectral-ratio method (Picotti and Carcione, 2006). We assume that the cut-off frequency to evaluate aliasing effects is 50 Hz.

The time-domain equations for propagation in a heterogeneous viscoelastic medium in the presence of a free surface can be found in Carcione(1992, 2007) and Carcione et al. (2005). The anelasticity is described by a single relaxation peak per mode and it is based on the Zener model. By modes we mean pure dilatational and shear deformations of the medium, such that the related Q factors are Q_k and Q_S, respectively. Q_k can be obtained from Q_P and Q_S (e.g., Carcione, 2007). The seismograms are computed with the Runge-Kutta method for time stepping and the Fourier and Chebyshev differential operators to compute the spatial derivatives in the horizontal and vertical directions, respectively. Chebyshev transforms are computed with the FFT, with a length twice of that used by the Fourier method. Since the sampling points are very dense at the edges of the mesh, the Chebyshev method requires a one-dimensional stretching transformation to avoid very small time steps (Carcione, 1992).

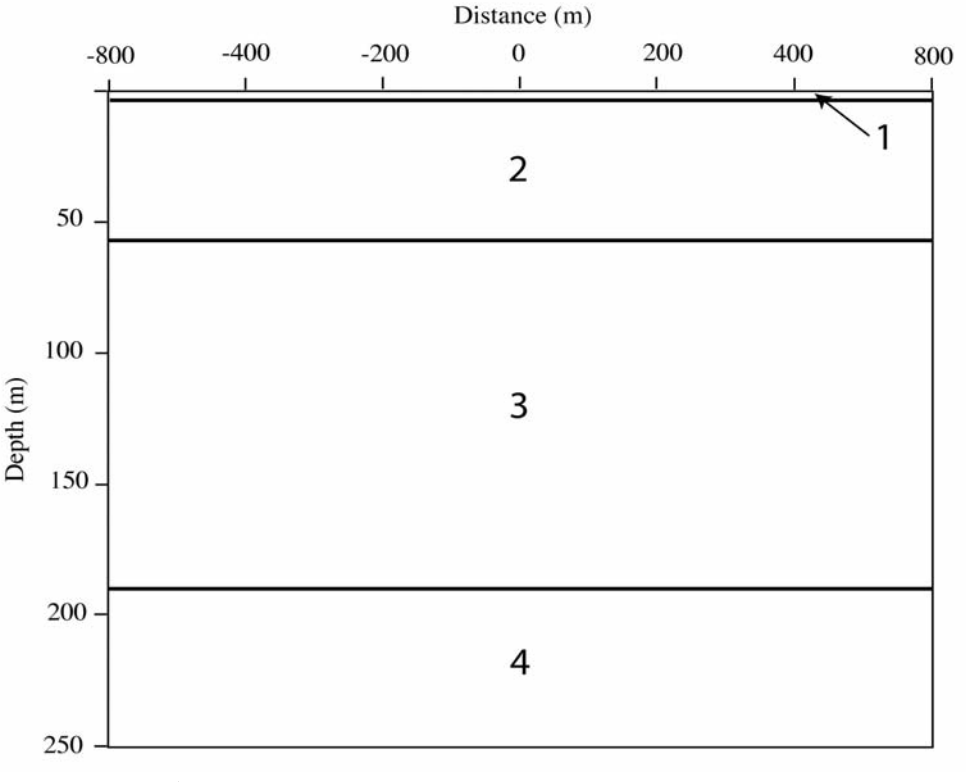

Fig. 6. Geological model interpreted from the common-shot gather shown in Fig. 2. Wave velocities, density and quality factors are indicated in Table 1.

Table 1. Layer Properties.

Layer	v_P (km/s)	v_S(km/s)	Q_P	Q_S	Q_k	ρ (kg/m^3)	Thickness (m)
1	0.38	0.22	14	11	19	1460	2
2	2	0.55	30	17	34	1960	55
3	2.8	1.245	35	25	42	2040	130
4	4.8	2.77	45	35	60	2700	∞

The source time history is

$$h(t) = (u - \tfrac{1}{2})\exp(-u) \quad , \quad \text{where } u = [\pi f_p(t - t_s)]^2 \quad , \tag{3}$$

t_p is the period of the wave and we take $t_s = 1.4t_p$. The peak frequency is $f_p = 1/t_p$ and the cut-off (maximum) frequency is $2f_p$.

The numerical mesh has 675 × 101 points with a grid spacing of 2 m in the horizontal direction and a vertical size of 470 m. Absorbing strips of 50 points length are used at the sides and bottom to prevent non-physical events from the boundaries. The source is a vertical force applied at the surface and has a dominant frequency f_p = 25 Hz. The source delay is t_s = 26 ms, which is the time lag of the peak with respect to the onset of the wavelet.The time step is 0.25 ms and the maximum propagation time is 0.8 s. Fig. 7 shows the seismogram of the vertical particle-velocity component. The Rayleigh-wave fundamental mode can be seen as the strongest event, followed by an S-wave reflection at the first interface. The reflection event "R" corresponds to the interface at 188 m (top of the basalt). Snapshots at 0.2 and 0.3 s are displayed in Fig. 8, where the events indicated in Fig. 7 are identified. The reverberations can clearly be appreciated and a strong S-wave reflection following the Rayleigh wave can be seen in Fig. 8b. This event is masked in the real data.

DISCUSSION

The purpose of the first preliminary seismic surveys has been to process the data with the standard processing technique in order to obtain a stacked section. However, this task could hardly be accomplished with good quality since the presence of surface waves mask the reflection events from the base of the shallower layer and interfere with deeper events. Surface waves are not properly spatially filtered in the field since the stations are composed of a single geophone and not geophone arrays (e.g., Yilmaz, 1989). However, by

interpreting a shot gather, we have obtained the depth of the first shallow layer and the elastic velocities, while the top of the basalt layer has been inferred from the stack.

It would be possible to extract group velocities from these seismograms using a multiple filter technique (Dziewonski and Hales, 1972). However, the design of the experiment requires a proper spacing between stations to avoid spatial aliasing (see Steeples and Miller, 1998). Fig. 9 shows two f-k transforms. The first (a) corresponds to the synthetic seismogram of Fig. 6 (geophone spacing is 10 m) and Fig. 9b refers to the same model but with a geophone spacing of 4 m. We did not considered the very low velocity thin layer to avoid time aliasing. We can see that the ground roll in Fig. 9a has been spatially aliased due to the large receiver spacing, while it is entirely preserved

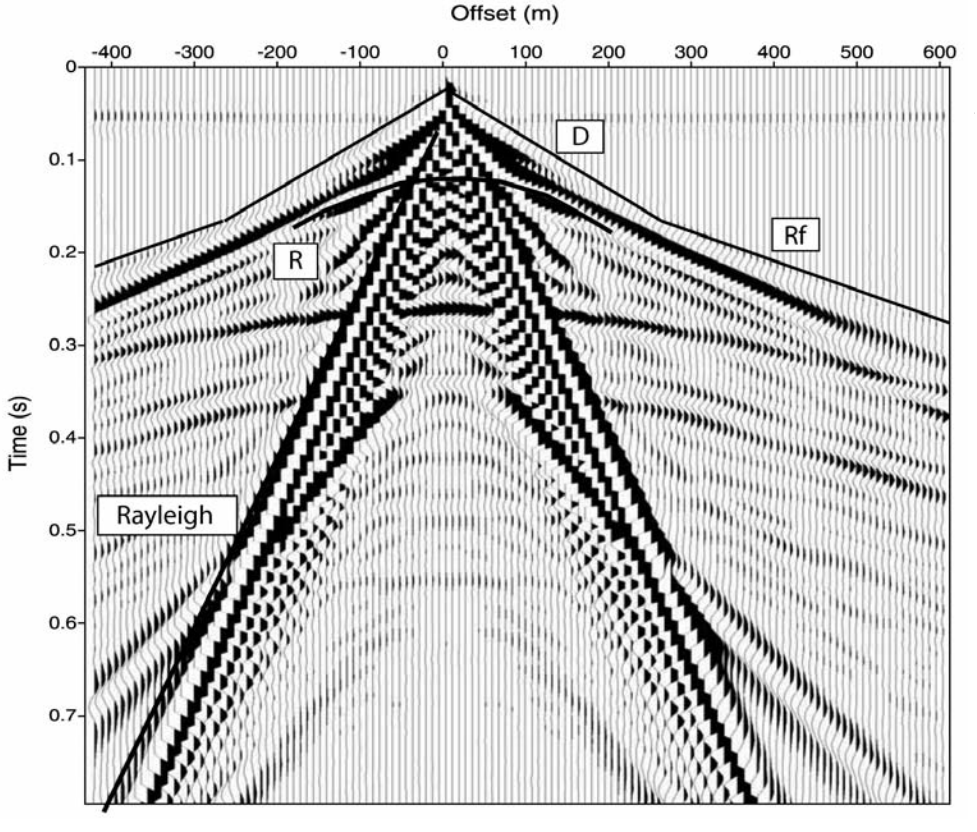

Fig. 7. Synthetic seismogram (common-shot) corresponding to the model shown in Fig. 6. The events are identified, where "R" corresponds to the reflection of the top of the basalt layer.

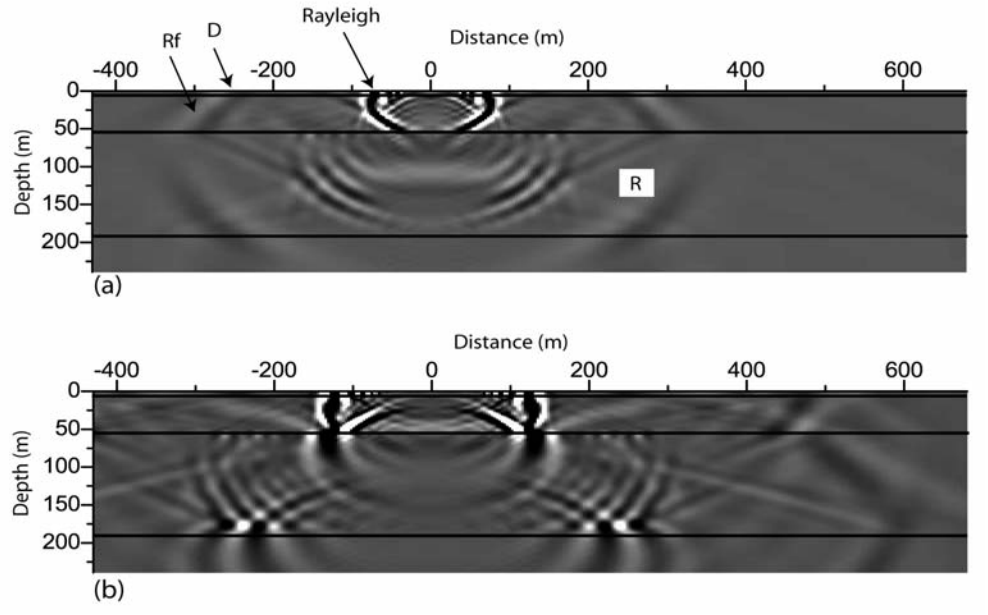

Fig. 8. Snapshot at 0.2 s and 0.3 s, corresponding to the model shown in Fig. 6. The interfaces and events are indicated.

in Fig. 9b. The choice of a smaller receiver distance and possibly a different source, such as a falling weight, could generate higher wavenumbers and frequencies and can give a better definition of the shallow interfaces (e.g., Hunter et al., 2000).

Other experiments to perform are refraction surveys that can be useful to locate the top of the basalt layer. The experiments require enough offset to clearly see the refracted waves from the first interface and the top of the basalt layer. The thicknesses of the interfaces can be computed recursively from the intercept times. The first is t_0 [see eq. (A-2)] and the intercept time of the second interface is

$$t_1 = T_0\sqrt{\{1 - (v_1^2/v_3^2)\}} + (2h'/v_2)\sqrt{\{1 - (v_2^2/v_3^2)\}} \quad , \tag{4}$$

where h' is the thickness of the second layer and v_3 is the P-wave velocity of the basalt layer. The velocities are obtained from the slopes of the curves and h' can be calculated from eq. (4). As a "rule of thumb", the depth of investigation for refraction seismic lines is typically about one-quarter to one-third the farthest offset. If this is 1000 m, the depth is 250 to 330 m.

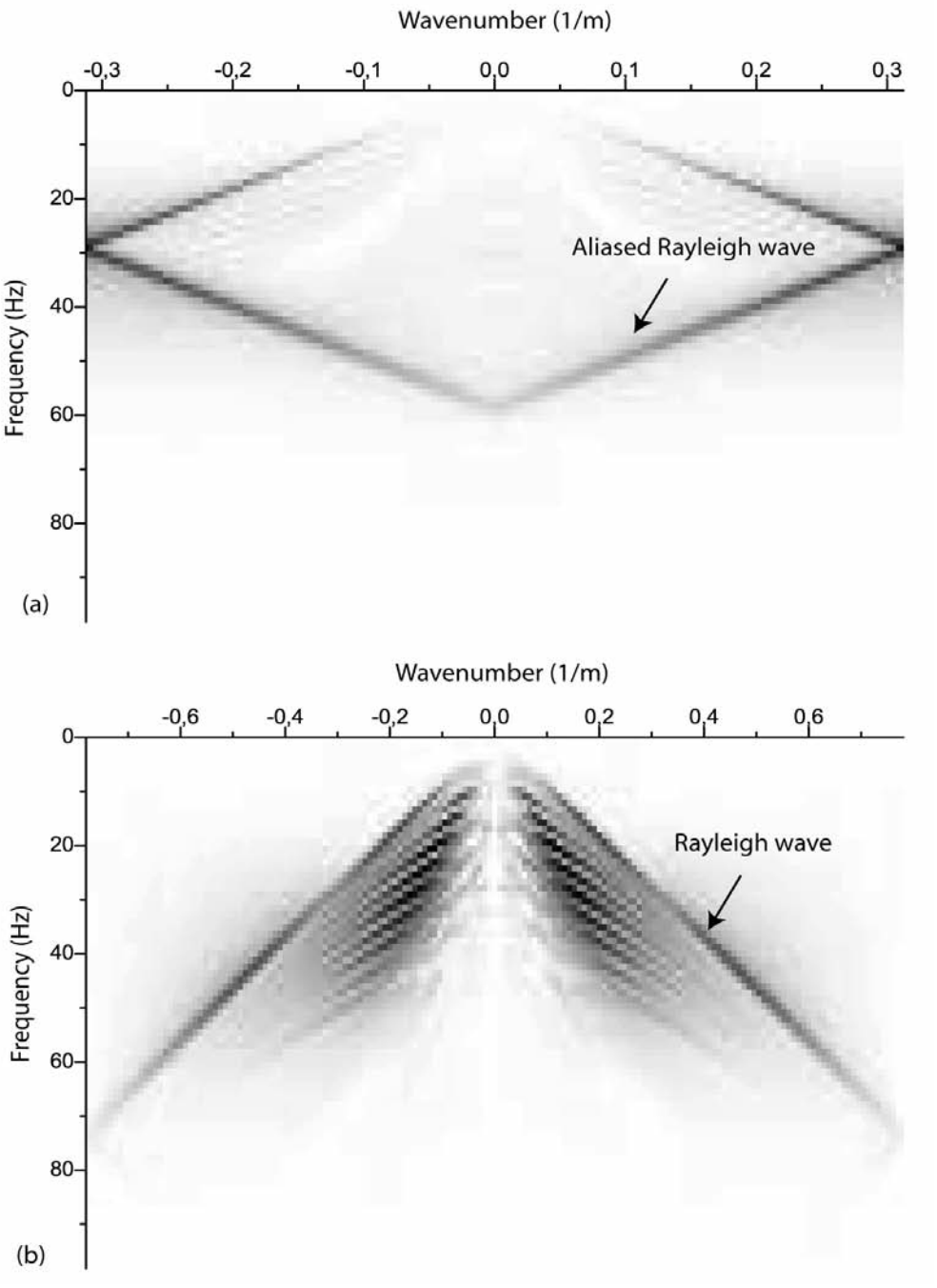

Fig. 9. f-k transform of the synthetic seismograms obtained from the model shown in Fig. 6, with $\Delta x = 10$ m (a) and $\Delta x = 4$ m (b).

The source/first-receiver offset can be varied on the basis of the depth of the target, but a large near offset should be avoided.It can be easily seen that the critically-refracted ray at the second interface emerges at the surface at

$$x_{c2} = 2h(v_1/v_3)\{1 - (v_1^2/v_3^2)\}^{-½} + 2h'(v_2/v_3)\{1 - (v_2^2/v_3^2)\}^{-½} \quad . \qquad (5)$$

To capture this emergence point, the near offset should be smaller than x_{c2}. For instance, this distance is x_{c2} = 241 m for the model shown in Fig. 6.

CONCLUSIONS

Seismic-reflection data from the Llancanelo-Lake area has been interpreted in the shot and post-stack domains. The analysis of a shot gather (traveltimes) provides the depth of the first interface and P-wave velocities of the two shallow layers, in addition to the S-wave velocity of the shallow layer inferred from rock-physics empirical relations and the Rayleigh waves. A very low velocity and thin surface layer can be deduced from the traveltimes and the presence of ringing in the events. Forward modeling simulations help to understand the nature of the different events and provide enough confidence about the interpretation. The geological model obtained from this procedure consists of two main layers composed of volcaniclastic sediments, with an interface between 50 and 60 m, overlying a basalt bedrock at 190 m approximately. The model is complemented with information obtained from the stacked section. The processing requires the suppression of the surface and refracted waves by frequency-wavenumber filtering. In particular, the removal of the direct and refracted waves also removes part of the medium and far-offset reflection signals, but it is necessary to avoid stacking refractions and misinterpreting very shallow related events as geological interfaces. The stack confirms the P-wave velocity profile and identifies the second interface hypothesized by analyzing the shot gather. Moreover, it reveals deeper interfaces.

ACKNOWLEDGEMENTS

This work was partially funded by ANPCyT, PICT 1311. The seismic-reflection data was stacked by using Seismic Unix software. We thank Prof. John Ferguson who provided useful comments.

REFERENCES

Carcione, J.M., 1992. Modeling anelastic singular surface waves in the Earth. Geophysics, 57: 781-792.

Carcione, J.M., 2007. Wave Fields in Real Media. Theory and numerical simulation of wave propagation in anisotropic, anelastic, porous and electromagnetic media, 2nd ed. Elsevier Science Publishers, Amsterdam.

Carcione, J.M., Helle, H.B., Seriani, G. and Plasencia, M.P., 2005. On the simulation of seismograms in a viscoelastic Earth by pseudospectral methods. Geophys. Internat., 44: 123-142.

de la Vega, M., Lopez, E., Osella, A., Rovere, E.I. and Violante, R.A., 2011. Quaternary stratigraphy and evolution of the Llancanelo lake region (Southern Mendoza, Argentina) evidenced from geoelectric methods. Submitted to Quatern. Res.

Dziewonski, A.M. and Hales, A.L., 1972. Numerical analysis of dispersed surface waves. In: Bolt, B.A. (ed.), Methods in Computational Physics, Vol. 11. Academic Press, New York.

Gil, A., Zarate, M. and Neme, G., 2005. Mid-Holocene paleoenvironments and the archeological record of southern Mendoza, Argentina. Quatern. Internat., 132: 81-94.

Greenhalgh, S.A. and King, D.W., 1981. Curved raypath interpretation of seismic refraction data. Geophys. Prosp., 29: 853-882.

Hunter, J.A., Burns, R.A., Aylsworth, J.M. and Pullan, S.E., 2000. Near-surface seismic-reflection studies to outline a buried bedrock basin in eastern Ontario. Geological Survey of Canada, Ottawa.

Mavko, G., Mukerji, T. and Dvorkin, J., 1998. The Rock Physics Handbook: Tools for Seismic Analysis in Porous Media. Cambridge Univ. Press, Cambridge.

Petrosino, S., Cusano, P., Saccorotti, G., Del Pezzo, E., 2002. Seismic attenuation and shallow velocity structures at Stromboli Volcano, Italy. Bull. Seismol. Soc. Am., 92: 1102-1116.

Picotti, S. and Carcione, J.M., 2006. Estimating seismic attenuation (Q) in the presence of random noise. J. Seismic Explor., 15: 165-181.

Pilant, W.L., 1979. Elastic Waves in the Earth. Elsevier Science Publishers, Amsterdam.

Ramos, V.A. and Folguera, A., 2011. Payenia volcanic province in the Southern Andes: An appraisal of an exceptional Quaternary tectonic setting. J. Volcanol. Geotherm. Res., 201: 53-64.

Risso, C., Németh, K., Combina, A.M., Nullo, F. and Drosina, M., 2008. The role of phreatomagmatism in a PlioPleistocene high-density scoria cone field: Llancanelo Volcanic Field (Mendoza, Argentina). J. Volcanol. Geotherm. Res., 169: 61-86.

Sheriff, R.E. and Geldart, L.P., 1995. Exploration Seismology. Cambridge University Press, Cambridge.

Steeples, D.W. and Miller, R.D., 1998. Avoiding pitfalls in shallow seismic reflection surveys. Geophysics, 63: 1213-1224.

Violante, R., Osella, A., de la Vega, M., Rovere, E. and Osterrieth, M., 2010. Paleoenvironmental reconstruction In the Western Lacustrine Plain of Llancanelo Lake, Mendoza, Argentina. J. South Am. Earth Sci., 29: 650-664.

Yilmaz, O., 1989. Seismic Data Processing. SEG, Tulsa, OK.

APPENDIX

REFLECTION AND REFRACTION RAY EQUATIONS

The mathematical expressions of the traveltime curves, corresponding to Fig. 3, are (Pilant, 1979; Sheriff and Geldart, 1995)

$$t_D = x/v_1 \ , \quad t_R = \sqrt{\{T_0^2 + (x^2/v_1^2)\}} \ , \quad t_{Rf} = (x/v_2) + t_0 \ , \tag{A-1}$$

where

$$t_0 = T_0\sqrt{\{1 - (v_1^2/v_2^2)\}} \ , \quad T_0 = 2h/v_1 \ , \quad t_c = T_0^2/t_0 \ . \tag{A-2}$$

The cross-over distance x_1 is found by setting $t_D = t_{Rf}$. It gives

$$x_1 = 2h\sqrt{\{(v_2 + v_1)/(v_2 - v_1)\}} \ , \tag{A-3}$$

and

$$x_c = 2h\tan\theta_c = (2v_1h/v_2)\{1 - (v_1^2/v_2^2)\}^{-½} \ . \tag{A-4}$$

The velocities v_1 and v_2 can be obtained from the slopes of the direct and refracted waves. The thickness of the layer can independently be computed from T_0, t_0, x_c or x_1 as

$$h = T_0v_1/2 = \{v_1\sqrt{(t_0t_c)}\}/2 \ , \quad h = \{t_0v_1/2\}\{1-(v_1^2/v_2^2)\}^{-½} \ ,$$

$$h = \{x_cv_2/2v_1\}\sqrt{\{1-(v_1^2/v_2^2)\}} \ , \quad h = (x_1/2)\sqrt{\{(v_2-v_1)/(v_2+v_1)\}} \ , \tag{A-5}$$

respectively.